In Vitro and in Vivo Evaluation of Ruthenium(II)−Arene PTA Complexes

Claudine Scolaro,[†] Alberta Bergamo,[‡] Laura Brescacin,[‡] Riccarda Delfino,[‡] Moreno Cocchietto,[‡] Gábor Laurenczy,[†] Tilmann J. Geldbach,[†] Gianni Sava,*[,‡,§] and Paul J. Dyson*[,†]

Institut des Sciences et Ingénierie Chimiques, Ecole Polytechnique Fédérale de Lausanne (EPFL), CH-1015 Lausanne, Switzerland, Callerio Foundation Onlus, Via A. Fleming 22−31, 34127 Trieste, Italy, and Dipartimento di Scienze Biomediche, Università di Trieste, Via L. Giorgieri 7-9, 34127 Trieste, Italy

Received January 7, 2005

The antitumor activity of the organometallic ruthenium(II)−arene complexes, $RuCl_2(\eta^6$-arene)-(PTA), (arene = *p*-cymene, toluene, benzene, benzo-15-crown-5, 1-ethylbenzene-2,3-dimethylimidazolium tetrafluoroborate, ethyl benzoate, hexamethylbenzene; PTA = 1,3,5-triaza-7-phosphaadamantane), abbreviated RAPTA, has been evaluated. In vitro biological experiments demonstrate that these compounds are active toward the TS/A mouse adenocarcinoma cancer cell line whereas cytotoxicity on the HBL-100 human mammary (nontumor) cell line was not observed at concentrations up to 0.3 mM, which indicates selectivity of these ruthenium(II)−arene complexes to cancer cells. Analogues of the RAPTA compounds, in which the PTA ligand is methylated, have also been prepared, and these prove to be cytotoxic toward both cell lines. RAPTA-C and the benzene analogue RAPTA-B were selected for in vivo experiments to evaluate their anticancer and antimetastatic activity. The results show that these complexes can reduce the growth of lung metastases in CBA mice bearing the MCa mammary carcinoma in the absence of a corresponding action at the site of primary tumor growth. Pharmacokinetic studies of RAPTA-C indicate that ruthenium is rapidly lost from the organs and the bloodstream.

Introduction

Current inorganic drugs such as cisplatin and related compounds are successfully used in the treatment of many cancer types with a high social incidence.[1,2] However there are problems associated with their use, in particular, cisplatin is highly toxic, leading to side effects and limiting the dose that can be administrated.[3] New developments in platinum drug design[4,5] and drug-dosing protocols[6] have gone some way to reduce the toxicity of these compounds. Complexes based on other metals have been investigated for their possible application as antitumor drugs. One of the most promising metals is ruthenium,[7,8] and a number of ruthenium complexes show high in vitro and in vivo antitumor activity and some compounds are currently undergoing clinical trials.[9−11] Although the mechanism of action of antitumor ruthenium compounds is not fully understood, it is thought that for certain species, similar to the platinum drugs, the chloride ligands are substituted by water in vivo,[12,13] which subsequently undergo substitution by the nucleobases of DNA.[14]

The ruthenium complex ImH[*trans*-$RuCl_4$(DMSO)Im], NAMI-A, has high selectivity for solid tumor metastases and low host toxicity at pharmacologically active doses[15] and was the first ruthenium complex to enter clinical trials.[16] Although this complex has a remarkably low general toxicity,[17,18] and shows marked efficacy against metastases,[19,20] it does not affect primary tumor growth[21−23] and does not exhibit cytotoxicity against tumor cells in vitro. A related ruthenium(III) compound, KP1019,[24] has also entered clinical trials, since it was found to exhibit antiproliferative activity in vitro in human colon carcinoma cell lines.[25]

The lower general toxicity of ruthenium complexes compared to platinum drugs has been attributed to the ability of ruthenium compounds to specifically accumulate in cancer tissues.[26] The higher specificity of these compounds for their targets may also be linked to the selective uptake by the tumor compared with healthy tissue[27,28] and because of a selective activation by reduction to cytotoxic species within the tumor.[29]

While the anticancer activity of ruthenium coordination complexes has been studied in detail for many years, organoruthenium compounds, with direct ruthenium−carbon bonds, are now attracting interest. The first organoruthenium compound to be evaluated as an anticancer agent was $Ru(\eta^6$-$C_6H_6)Cl_2$(metronidazole) (metronidazole = 1-β-hydroxyethyl-2-methyl-5-nitroimidazole). While it was found that the complex had a greater selective cytotoxicity than metronidazole itself under hypoxic reducing conditions, as far as we are aware, further studies were not forthcoming.[30] Subsequently, several types of ruthenium(II)−arene complexes have shown high in vitro and/or in vivo antitumor activity including those with phosphine, amine, and sulfoxide co-ligands. Cationic $[RuCl(\eta^6$-arene)(en)$]^+$ (en = ethylenediamine) complexes show in vitro inhibition of cancer cell growth and in vivo antitumor activity.[31,32] Although the interactions of the ruthenium(II)−arene compounds have been most extensively studied with DNA, $RuCl_2(\eta^6$-$C_6H_6)$(dimethylsulfoxide (DMSO) has been shown to inhibit the DNA relaxation activity of topoisomerase II.[33] Another series of ruthenium(II)−arene compounds with disulfoxide ligands have been

* Corresponding Author: Prof. Paul J. Dyson. E-mail: paul.dyson@epfl.ch. Tel: +41 (0)21 693 98 54. Fax: +41 (0)21 693 98 85.
† Institut des Sciences et Ingénierie Chimiques, Ecole Polytechnique Fédérale de Lausanne.
‡ Callerio Foundation Onlus.
§ Dipartimento di Scienze Biomediche, Università di Trieste.

10.1021/jm050015d CCC: $30.25
Published on Web 05/21/2005

Scheme 1. Protonation of the PTA Ligand in **1**, Postulated as Being Responsible for pH Dependant Damage to DNA

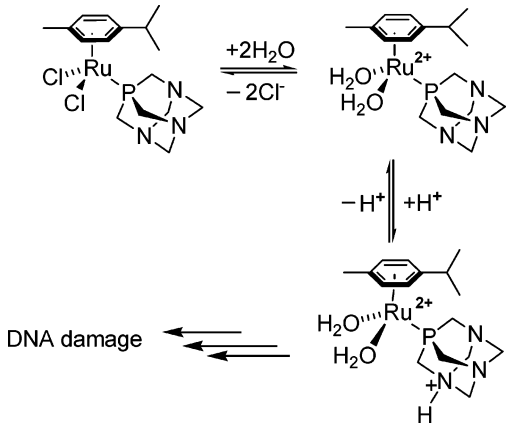

tested for anticancer activity in vitro and showed cytotoxicity against a human mammary cancer cell line.[34]

Our attention has focused on ruthenium(II)−arene complexes combined with the 1,3,5-triaza-7-phosphaadamantane (PTA) ligand. The compound $RuCl_2(\eta^6\text{-}C_{10}H_{14})$(PTA), named RAPTA-C, **1**, was found to exhibit pH-dependent DNA damage such that at the pH typical of hypoxic tumor cells, DNA was damaged, whereas at the pH characteristic of healthy cells, little or no damage was detected.[35,36] Such behavior was attributed to the PTA ligand which can be protonated at low pH, and the protonated form was considered to be the active agent. To test this hypothesis a detailed investigation of RAPTA compounds, as well as model Me-PTA analogues, has been undertaken, paying particular attention to their aqueous chemistry and in vitro cytotoxicity on tumor cells.[37,38] In parallel, in vivo experiments were carried out to evaluate the anticancer and antimetastatic activity of these complexes and the distribution of **1** in the organs and the blood. Herein, we describe the outcome from these studies.

Results and Discussion

We previously reported the synthesis, characterization, and effect of **1** on plasmid DNA.[35] It was found that at a pH >7 almost no damage to the DNA is observed, whereas below pH 7 DNA damage is prevalent. Since healthy cells grow at pHs above 7, typically pH 7.2, and (hypoxic) cancer cells have characteristically lower pH values, typically pH 6.8, we proposed that the compound might selectively target cancer cells. At the time, we proposed that PTA could be protonated at lower pH and in this form cause damage to the DNA as illustrated in Scheme 1.

With this mechanism in mind, we proposed that the methylated PTA derivative $[RuCl_2(\eta^6\text{-}C_{10}H_{14})(PTA\text{-}Me)]^+$ (**2**) would display indiscriminate DNA damage and show no specific selectivity toward cancer cells over healthy cells. To test this hypothesis, and consolidate the preliminary data obtained using plasmid DNA, cell studies were undertaken. RAPTA compounds **1**−**9** (see Chart 1) were prepared according to the method previously outlined for **1**. Full synthetic details and spectroscopic characterization is provided in the Experimental Section and in the Supporting Information.

Hydrolysis of 1 in Aqueous, Buffered, and Salt Solutions. To delineate the differences in activity between the RAPTA compounds and the methyl-PTA derivatives **2** and **4** it is important to know the identity of the compound that reaches the cell, and accordingly, the aqueous chemistry of the complexes is very important. Hydrolysis of **1** was studied using UV−vis spectrophotometry under various conditions. The UV−vis spectrum of **1** at 298 K immediately after dissolution in pure water exhibits a strong absorption band at 342 nm which rapidly changes (over several minutes) to 326 nm (see Figure 1) indicating that rapid hydrolysis of the complex takes place, although the exact nature of the hydrolysis product was not characterized until later (see below).

A similar approach was adopted to study the hydrolysis of **1** in phosphate buffered solutions at pH 2, 7, and

Chart 1. Structure of the Ruthenium(II)−arene−PTA (RAPTA) Compounds and the Me-PTA Derivatives of RAPTA-C and RAPTA-T, Prepared as the Chloride Salts

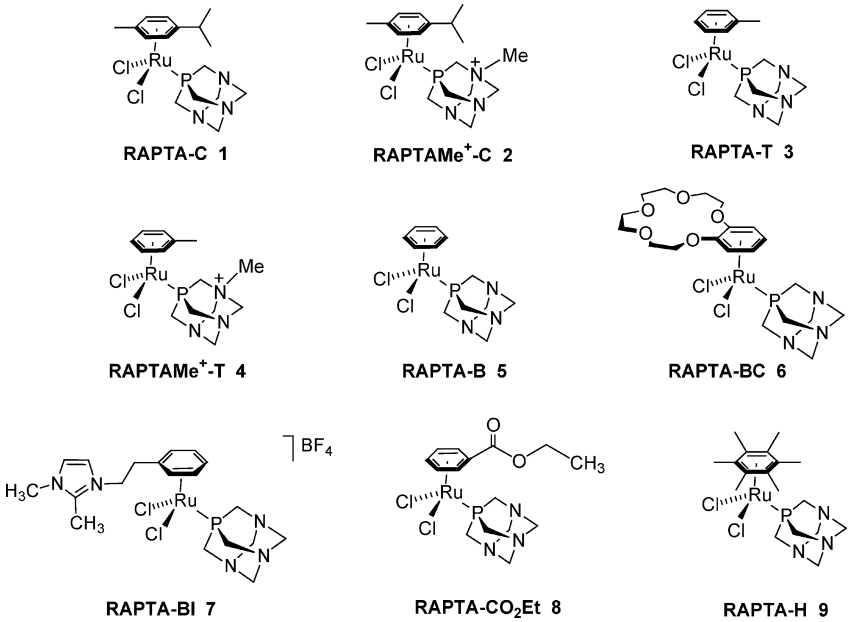

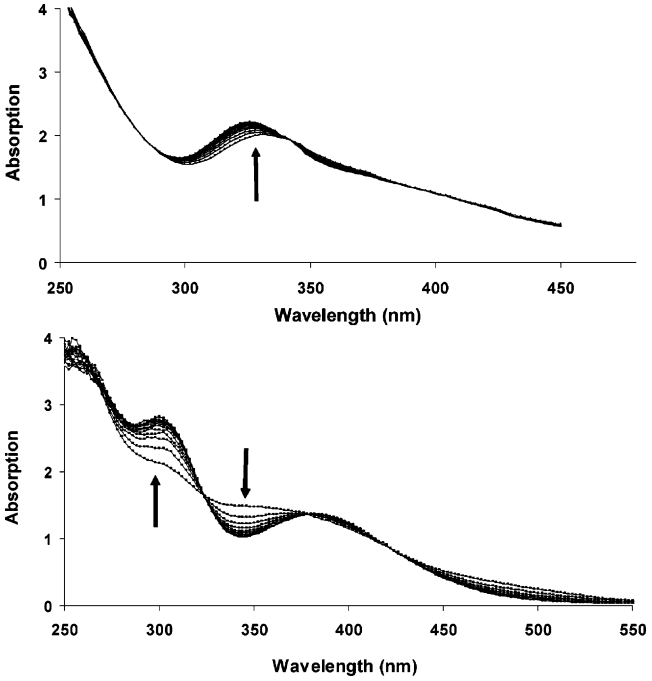

Figure 1. (Top) Time evolution of the UV−vis absorption spectra of **1** in water at 25 °C recorded at 1 min intervals over a period of 20 min (no further change was observed after this time). (Bottom) UV−vis absorption spectra of **1** in phosphate solution at pH 7, recorded every minute at 25 °C.

12 and in NaCl solutions representative of blood plasma (100 mM) and intracellular (4 mM) concentrations. In phosphate buffer solution at pH 2, essentially the same species is formed as that observed in water, as is demonstrated by the isosbestic point at 346 nm. Surprisingly, at pH 7, the spectrum (see Figure 1) is different from that observed in water and is similar to that determined in phosphate buffer at pH 12, indicating that the phosphate interacts with the complex. The initial absorption band at 342 nm, which corresponds to the dichloro compound, decreases with time and a species which absorbs at 300 nm is formed, and this equilibrium is characterized by an isosbestic point at 324 nm.

The UV−vis spectrum of **1** at 298 K in 4 mM NaCl solution is essentially the same as that observed in water, whereas in a 100 mM NaCl solution hydrolysis of **1** does not take place, that is, no change is observed in the UV−vis spectrum. These latter results indicate that the hydrolysis of **1** only takes place inside the cells where the chloride concentration is approximately 4 mM, whereas hydrolysis is suppressed at an extracellular concentration of chloride. Moreover, the maximum absorption band in the spectrum of **1** with 100 mM NaCl is similar to the spectrum obtained in dichloromethane which indicates that the compound is not hydrolyzed. These results suggest that the compound is only activated by hydrolysis inside the cell by substitution of chloride by water which then allows the compound to, for example, react further with DNA.

The identity of the hydrolysis product of **1** could not be ascertained from the UV−vis studies, and it is feasible that one or both of the chloride ligands could be replaced by water. Attempts to characterize the hydrolysis product using ^{17}O enriched water were unsuccessful. Thus, ionic chromatography was used to

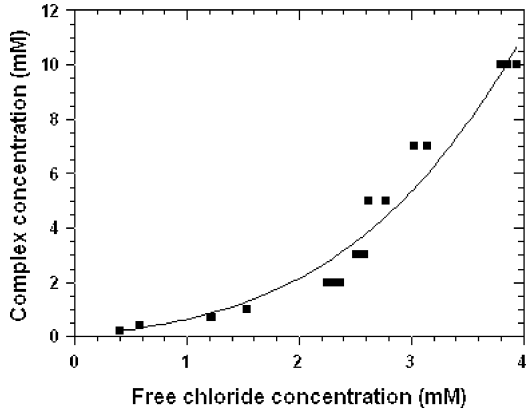

Figure 2. Determination of the free chloride concentration in an aqueous solution of complex **1** by ionic chromatography at 298 K.

Scheme 2. Proposed Hydrolysis of **1**

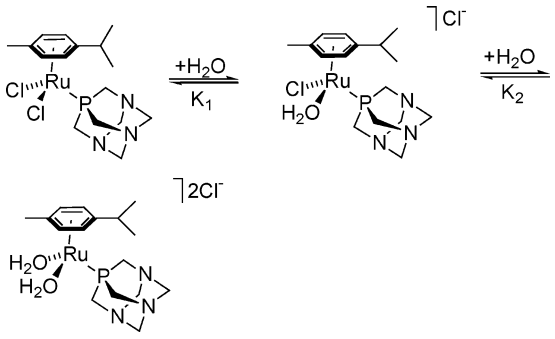

measure the concentration of chloride in aqueous solution to determine the extent of hydrolysis. A graph showing the concentration of the complex **1** vs the free chloride concentration measured in the solution is shown in Figure 2.

Somewhat unexpectedly, it was found that if one chloride is lost from **1**, then the second is also lost simultaneously, as indicated by the two equilibrium constants $K_1 = 0.03$ mM and $K_2 = 107$ mM at 298 K (see Scheme 2). However, loss of the chlorides is strongly dependent on the concentration of chloride present in solution. According to Scheme 2, an excess of free chloride displaces the equilibria to the left. The hydrolysis of **1** takes place relatively rapidly, and afterward there is no further change in the chloride concentration for several days. The equilibrium constants K_1 and K_2 were calculated from the total complex and free chloride concentrations using the least-squares fit method (the sum of squares of the difference (measured [chloride] − calculated [chloride]) were minimized).

This behavior is markedly different from that observed for cisplatin, which like **1** does not undergo hydrolysis in the extracellular medium, but rapidly loses one chloride for water once inside a cell, with the second hydrolysis step being considerably slower.[39] With ruthenium drugs, or drug candidates, hydrolysis also appears to be an important part of their activation. For example, the degradation of NAMI-A consists of stepwise hydrolysis of the chloride ligands in acidic media, accompanied by the hydrolysis of the DMSO group, followed by the formation of a poly-oxo species.[40] The coordinated water in $[Ru(OH_2)(\eta^6\text{-}p\text{-cymene})(en)]^{2+}$ deprotonated to the hydroxo species $[Ru(OH)(\eta^6\text{-}p\text{-cymene})(en)]^{+}$, and the respective acid dissociation constants of

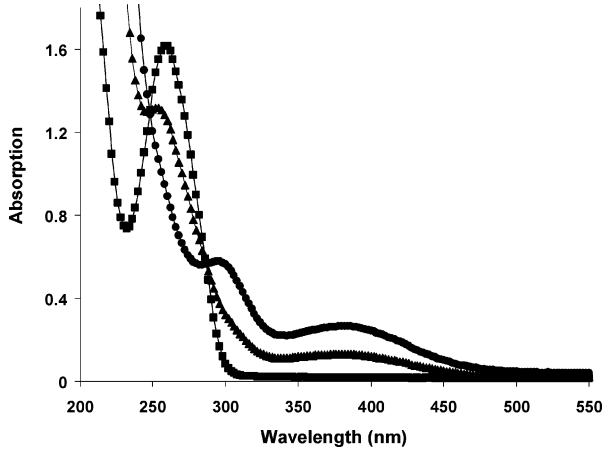

Figure 3. UV−vis absorption spectrum of **1** in water (●) and in a solution of calf thymus DNA (▲) overlaid with the calf thymus DNA spectrum (■).

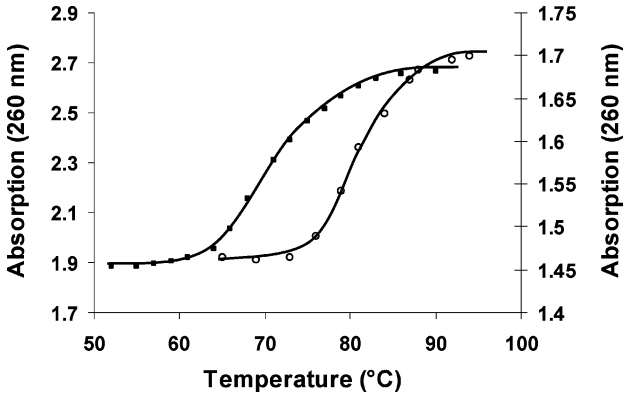

Figure 4. DNA melting curves of calf thymus DNA alone (■) and calf thymus DNA with **1** (1:1 ratio) (○). Buffer consisted of 10 mM phosphate buffer and 50 mM $NaClO_4$.

the aqua adducts were determined,[41] whereas in [Ru$(OH_2)_2(\eta^6$-arene)(PTA)]$^{2+}$ no such transformation had been observed under physiological pH values (see below).

DNA Interactions. The absorption spectra of calf thymus DNA, **1**, and a mixture of the two (1:1 ratio) are illustrated in Figure 3. Calf thymus DNA and **1** have overlapped transitions below 300 nm. Consequently, any metal complex spectral changes can be observed above 300 nm where calf thymus DNA has no absorbance. Effectively, when **1** is incubated with calf thymus DNA a change in the absorption spectra is observed, indicating that the compound binds to DNA. The melting of calf thymus DNA was studied in the presence of complex **1**. The increase in absorbance at 260 nm was recorded from 50 to 90 °C, and the melting temperature, T_m, was then determined from the denaturation curves shown in Figure 4.

Complex **1** is able to modify in vitro calf thymus DNA with the melting temperature increasing from 67 to 80 °C (ΔT_m = 13 °C) upon binding of the compound (see Figure 4). These data indicate that complex **1** induces a stabilization of the double helix with a corresponding increase in melting temperature. The effect of **1** on calf thymus denaturation can be compared to other ruthenium antitumor compounds. For example, the ruthenium(III) compounds, Na[*trans*-$RuCl_4$(DMSO)(Im)] (NAMI) and Ru(PDTA)Cl_2 (PDTA = propylenediaminetetraacetate), both induce a slight stabilization of the double helix ($\Delta T_m \approx +1-2$ °C).[42] The ruthenium(II)−arene complex $RuCl_2(\eta^6$-C_6H_6)(DMSO) induces a stabilization of the double helix between 9 and 23 °C depending on the concentration of the complex.[33]

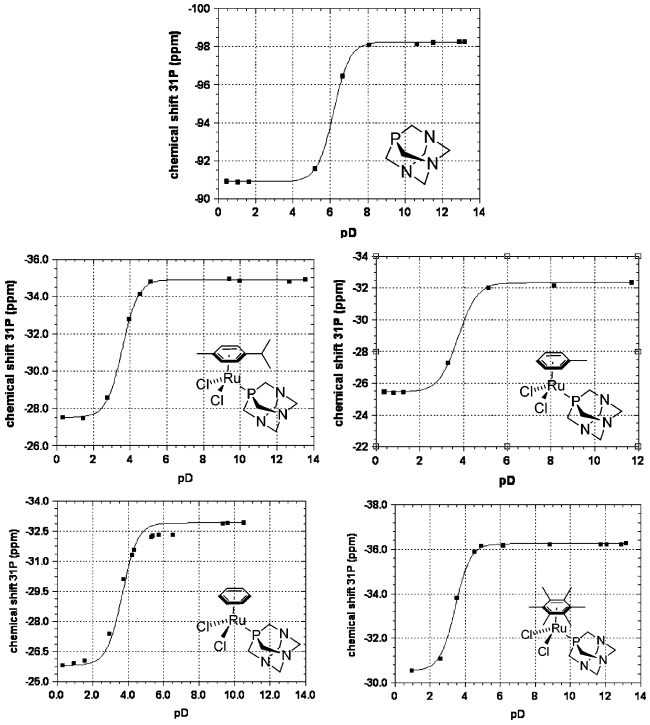

Figure 5. ^{31}P chemical shift vs p*D* for PTA (top), **1** (middle left), **3** (middle right), **5** (bottom left), and **9** (bottom right).

Table 1. pK_a Values for the PTA Ligand and for Complex **1**, **3**, **5,** and **9** at 298 K in 0.1 M NaCl Solution

complex	pK_a
PTA	5.63 ± 0.05
$RuCl_2(\eta^6$-$C_{10}H_{14})$(PTA), **1**	3.13 ± 0.02
$RuCl_2(\eta^6$-$C_7H_8)$(PTA), **3**	3.31 ± 0.03
$RuCl_2(\eta^6$-$C_6H_6)$(PTA), **5**	3.23 ± 0.06
$RuCl_2(\eta^6$-$C_6Me_6)$(PTA), **9**	2.99 ± 0.02

Protonation of the Phosphine PTA Ligand (pK_a). The pK_a of PTA, PTA-Me$^+$, and complexes **1**, **3**, **5**, and **9** was determined using ^{31}P NMR spectroscopy in D_2O (see Experimental Section). Graphs showing the chemical shift of the ^{31}P nucleus vs p*D* are shown in Figure 5, since no pK_a was observed for the methylated PTA compounds. The curves were fitted with the Henderson−Hasselbach equation. The pH titration curves were carried out in D_2O, and the pK_a value is obtained from the midpoint of the curve where 0.44 are subtracted.[43]

The pK_a values of the free and coordinated ligand are summarized in Table 1. The pK_a of PTA has been reported on more than one occasion with values of 6.0[44] and 5.7,[45] which are in keeping with those estimated herein. Upon coordination, the pK_a of the PTA ligand decreases, and it can be fine tuned by varying the arene ligand. These values were determined in the presence of chloride to ensure that the process being determined is the protonation of the PTA ligand attached to the complex. However, essentially identical values are also obtained in the absence of chloride, and the formation of hydroxo ligands from the hydrolyzed species was not observed.

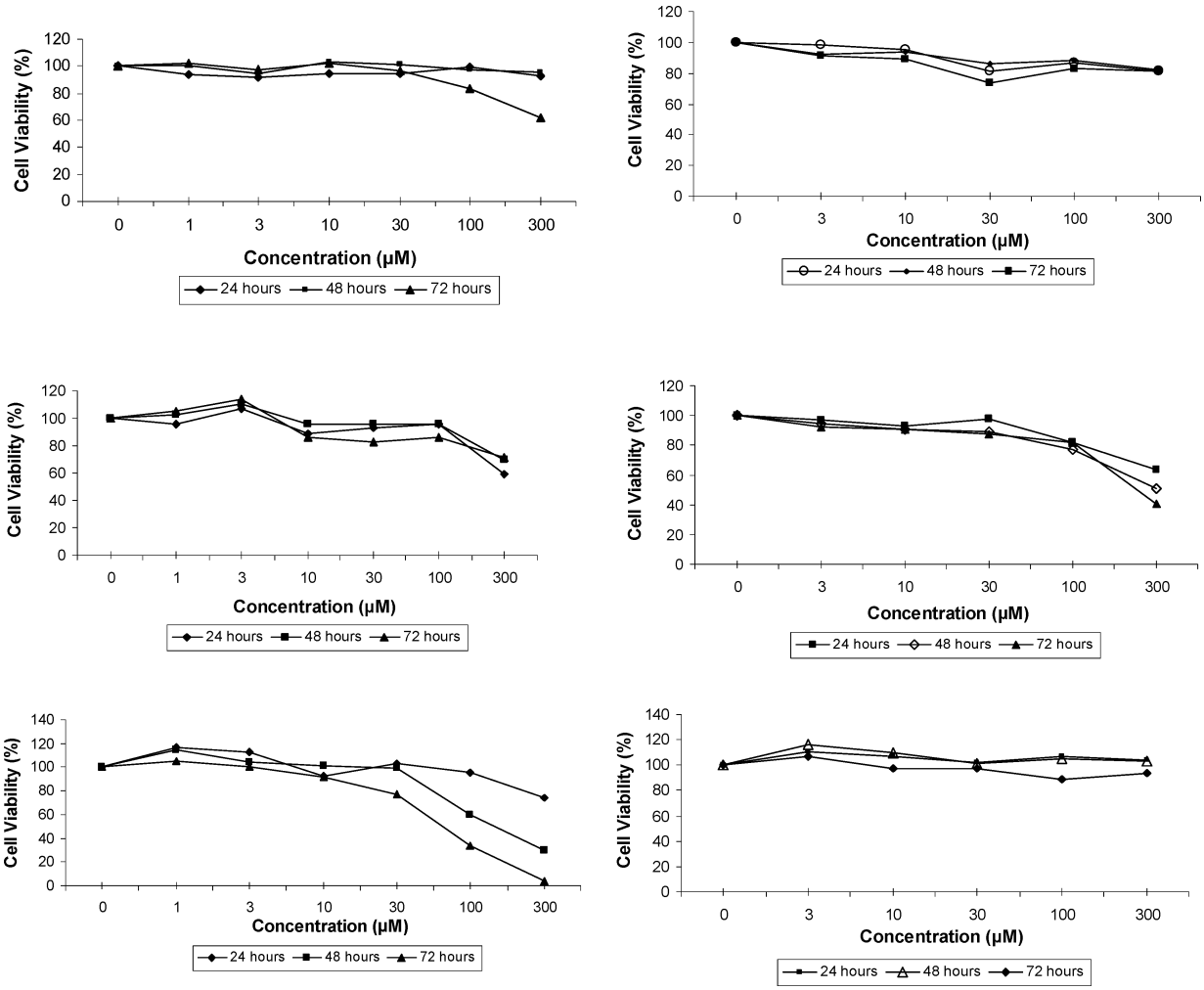

Figure 6. Effects of **1** on TS/A (top left) and HBL-100 (top right) cell proliferation, **2** on TS/A (middle left) and HBL-100 (middle right) cells, and **3** on TS/A (bottom left) and HBL-100 (bottom right). The cells were sown on day 0 and treated on day 1 with a range of concentrations between 1 and 300 μM, for the TS/A cells and HBL-100, of compound dissolved in water for 24, 48, and 72 h. The cell number was evaluated using the MTT test at the end of the treatment. Standard error bars (always below 10% of the mean values) are omitted for clarity.

These results indicate that a more complicated mechanism is required to rationalize the selective anticancer activity of RAPTA compounds. It is possible that once the complexes bind to DNA the pK_a of the PTA ligand increases to a value which is compatible with its protonation in the hypoxic environment of a cancer cell, which then exerts a secondary hydrogen bonding interaction much in the same way as cisplatin.[46] Combined, the two interactions may induce greater toxicity than coordination alone, but further experiments are required to prove such a hypothesis. However, protonation of the PTA ligand represents only one possible reason for the selectivity of the RAPTA compounds, and it is worth noting that while DNA is viewed as the traditional target for inorganic drugs, there is a great deal of evidence to suggest that for ruthenium compounds other non-DNA targets are important, and in the case of DNA targets many different kinds of DNA adducts can be formed with the anticancer agents. For example, the most prevalent DNA adduct with cisplatin is a linking of platinum to adjacent purine bases.[47] When cisplatin is allowed to react with DNA in vitro, the main adducts formed are 1,2-intrastrand cross-links, monofunctional adducts, or protein−DNA cross-links.[48,49] The possibility of drug interactions with proteins on the cell membrane in the understanding of antitumor activity of some anticancer compounds is a consideration that must be taken into account in further investigations.

Cytotoxic Effects on TS/A Adenocarcinoma Cells and on HBL-100 Mammary Cells. The biological 3-(4,5-dimethylthiazol-2-yl)-2,5-diphenyltetrazolium bromide (MTT) test which measures mitochondrial dehydrogenase activity as an indication of cell viability was carried out with all nine of the RAPTA compounds (see Chart 1) using two different cell lines, tumor mouse TS/A cells and normal human HBL-100 cells. The effects of ruthenium(II)−arene compounds **1**−**9** on the viability of these cells were evaluated by measuring the variations after 24, 48, and 72 h of treatment. The cell viability after these times was determined using the MTT assay, and the results from these studies are summarized in Figure 6 for RAPTA-C, its Me-PTA derivative **2**, and the toluene analogue **3**. The experiments were repeated twice for all of the compounds, and the IC_{50} values resulting from an average over the two experiments are listed in Table 2.

From Table 2 it is apparent that the RAPTA compounds **3** and **7** are clearly more cytotoxic for the cancer cells (TS/A) than for the normal cells (HBL-100) which suggest that they may be selective toward cancer cells

Table 2. IC_{50} Values of the RAPTA Compounds **1**, **3**, **5**, **6**, **7**, **8,** and **9** and Their Methyl-PTA Analogues **2** and **4** on the TS/A and HBL-100 Cell Lines after 72 h of Incubation

compound	IC_{50} (TS/A) 72 h (μM)	IC_{50} (HBL-100) 72 h (μM)
$RuCl_2(\eta^6\text{-}C_{10}H_{14})$(PTA), **1**	>300	>300
$[RuCl_2(\eta^6\text{-}C_{10}H_{14})$(Me-PTA)$]^+$, **2**	>300	246
$RuCl_2(\eta^6\text{-}C_7H_8)$(PTA), **3**	74	>300
$[RuCl_2(\eta^6\text{-}C_7H_8)$(Me-PTA)$]^+$, **4**	110	77
$RuCl_2(\eta^6\text{-}C_6H_6)$(PTA), **5**	231	>300
$RuCl_2(\eta^6$-benzo-15-crown-5)(PTA), **6**	159	>300
$[RuCl_2(\eta^6\text{-}C_6H_5(CH_2)_2Im)(PTA)][BF_4]$, **7**	66	>300
$RuCl_2(\eta^6\text{-}C_6H_5CO_2Et)$(PTA), **8**	103	>300
$RuCl_2(\eta^6\text{-}C_{12}H_{18})$(PTA), **9**	199	>300

in vivo, possibly leading to low toxicity. Most of the IC_{50} values could not be determined because the values are out of the concentration range used for the experiments and would be higher than 300 μM. The only two compounds which showed a measurable cytotoxicity for the normal cells are the methyl-PTA derivatives of RAPTA-C and RAPTA-T, both being slightly more toxic to the healthy cells. All of the other compounds can be considered as nontoxic toward the HBL-100 cells. Even the functionalized compounds **6** and **7** exhibit selective toxicity toward the cancer cells.

The most striking difference in cytotoxicity between the two cells lines is observed for **3** and **7** which exhibit IC_{50} values of 74 and 66 μM after 72 h of incubation with the TS/A adenocarcinoma cells but are essentially nontoxic to the HBL-100 normal cells under analogous conditions. Moreover, the cytotoxicity of RAPTA-T **3** shows activity dependence with the time of exposure (see Figure 6). A similar pattern is observed for the *p*-cymene analogue **1**, but it is less effective toward the cancer cells than the toluene analogue. The selective cytotoxicity of the RAPTA compounds toward the cancer cells could potentially lead to a drug with lower side effects compared to other metal-based anticancer drugs. However, it is worth noting that all of the series of RAPTA compounds are less active than cisplatin where the MTT assay using the same cell line (TS/A) gave a corresponding IC_{50} of 0.53 μM, although cisplatin displays a very high general cytotoxicity.[50,51] Other ruthenium(II)−arene compounds have been tested on the human mammary cancer cell line (MDA-MB-435s) and the human ovarian cancer cell lines and exhibit IC_{50} values between 55 and 360 and 6−200 μM,[34] respectively, which is in keeping with the compounds described herein and characteristic of ruthenium compounds which are generally less cytotoxic than platinum compounds. Another series of ruthenium(II)−arene complexes have been evaluated for activity in vitro against the platinum-sensitive human ovarian cancer cell line A2780 which showed high cytotoxicity with IC_{50} values between 0.5 μM and 100 μM, some being comparable to carboplatin and cisplatin antitumor agents.[31,32] These complexes seem to act in the same way as the cytotoxic agent, cisplatin, that is, via DNA binding. However, the antimetastatic NAMI-A complex does not show direct cytotoxicity for tumor cells in vitro, but it is highly effective in vivo against metastasis cells. Its mode of action is consistent with antiangiogenic properties, inhibition of matrix metalloproteinase, and modulation of tumor−tissue interactions.[28,52]

Determination of Intracellular Ruthenium Concentration. After TS/A cells were exposed to 100 μM of RAPTA compounds for 24 h, their uptake was determined by flameless atomic absorption spectroscopy (AAS), and the results are reported in Table 3.

Table 3. Ruthenium Uptake after Treatment for 24 h in TS/A Cells in Vitro with 100 μM of RAPTA Compounds

compounds	intracellular RAPTA ($\mu g/10^6$ cells)	intracellular RAPTA ($\times 10^{-4}$ M)
RAPTA-C, **1**	0.12 ± 0.02[a]	2.55 ± 0.06
RAPTA-B, **5**	0.13 ± 0.02	3.26 ± 0.04
RAPTA-H, **9**	0.15 ± 0.01	3.16 ± 0.27
RAPTA-T, **3**	0.16 ± 0.02	2.9 ± 0.3
RAPTA-BI, **7**	0.19 ± 0.04	3.03 ± 0.67
RAPTA-BC, **6**	0.28 ± 0.02	4.63 ± 0.35
$RAPTAMe^+$-T, **4**	0.33 ± 0.08	5.9 ± 1.4
RAPTA-CO_2Et, **8**	3.40 ± 0.41	54.67 ± 6.66

[a] Each number is the mean ± SE of an experiment made in triplicate.

Under the conditions used, the intracellular concentration of ruthenium is 2- to 6-fold higher for all of the RAPTA compounds when compared to the concentration in the culture medium. The amount of ruthenium in the tumor cells is between 0.12 and 0.33 μg with the exception of **8** where the intracellular concentration is 54.67×10^{-4} M corresponding to 3.40 μg of ruthenium per million cells. A reasonable hypothesis for explaining the high amount of **8** in the tumor cells after only 24 h of incubation may be the presence of esterases which break the ester function such that the resulting charged species remain inside the cell.[53] The RAPTA compounds may enter the tumor cells either by passive diffusion or by active transport, or even by an association of these two processes, but without further experiments it is not possible to say explicitly which mechanism is involved.

Effects on Tumor Growth and Metastases Formation. In vivo experiments were carried out with **1** and **5** to evaluate the effects of these compounds on primary tumor growth and lung metastasis formation, using the MCa mammary carcinoma in CBA mice, with ip (intraperitoneal) treatment started 5 days after tumor implantation. The control group consisted of nine mice. The tested groups with **1** contained five mice each. Different doses of compound were used for each group of five mice to establish the presence of a dose−effect relationship. The first group received a single dose of 200 mg/kg on day 5 after tumor implantation. This injection was also performed on another group with a second injection on day 9. Another group received a dose of 100 mg/kg on days 5, 7, 9, and 11. The total dose of 400 mg/kg was also divided into a daily injection of 40 mg/kg from days 5 to 14. The last treated group was given a single injection of 400 mg/kg. The experiment ended on day 20 after which tumor growth and lung metastases were counted. The effects of **1** on the primary tumor and lung metastasis formation are reported in Table 4.

For RAPTA-B **5**, the experiment comprised two treated groups of mice and the control group. The first group received a daily injection of 40 mg/kg from days 5 to 14 and the second group a dose of 100 mg/kg on days 5, 7, 9, and 11. The experiment ended on day 19 and lung metastases were counted. The effects of **5** on the volume of the primary tumor and lung metastases formation are shown in Table 5.

The in vivo experiment where **1** was administrated shows diverse behaviors depending on the schedule of

Table 4. Effects of **1** on the Tumor Growth and Metastasis Formation of MCa Mammary Carcinoma in CBA Mice

RAPTA-C **1**		lung metastases[b]	
treatment group	primary tumor[a] (mg)	no.	weight
controls	3780 ± 164	14.6 ± 4.5	29.5 ± 8.8
200 mg/kg	3498 ± 233	13.3 ± 9.9	19.6 ± 18.9
200 mg/kg/day (×2)	3663 ± 160	6.3 ± 3.5	21.4 ± 9.6
100 mg/kg/day (×4)	3472 ± 161	7.3 ±2.1	18.7 ± 6.3
40 mg/kg/day (×10)	4173 ± 215	12.8 ± 4.3	21.1 ± 8.6
400 mg/kg/day	3442 ± 164	19.7 ± 8.1	34.9 ±12.5

[a] Measured on day 19. [b] Measured on day 20.

Table 5. Effects of **5** on the Tumor Growth and Metastasis Formation of MCa Mammary Carcinoma in CBA Mice

RAPTA-B **5**		lung metastases[a]	
treatment group	primary tumor[a] (mg)	no.	weight
controls	3776 ± 352	15.8 ± 3.7	4.7 ± 1.8
40 mg/kg/day (×10)	3038 ± 398	11.6 ± 2.7	2.8 ± 1.0
100 mg/kg/day (×4)	3376 ± 194	11.5 ± 2.1	3.3 ± 1.4

[a] Measured on day 19.

administration. RAPTA-C **1** was found to reduce the number of lung metastases when given at 2 × 200 and 4 × 100 mg/kg/day schedules. The single dose of 400 mg is totally devoid of effects (see Table 4). The dose of 200 mg/kg repeated twice appears to be the most efficient in reducing lung metastases formation. It is important to note that at the end of the experiment when the metastases were counted, two mice (out of five) in this treated group did not have any metastasis. From these observations, it seems that the single dose of 400 mg/kg is too large, but if the injection is divided into 2 doses of 200 mg/kg the effect on lung metastases formation is more significant. Effectively, the results obtained with the other dose (4 × 100 mg/kg/day) administrated with higher frequency also show similar effects on lung metastases formation.

RAPTA-B **5** was also studied in the same mouse model administered with a total dose of 400 mg/kg at two different frequencies, and the effects of this complex on the primary tumor growth and on lung metastases formation are reported in Table 5. The two different doses of **5** administrated to the mice have the same slight, statistically nonsignificant, effect on the metastases number. Moreover, these two doses do not influence the evolution of the primary tumor.

NAMI-A, given ip at 35 mg/kg/day for 6 consecutive days, to mice bearing MCa mammary carcinoma, Lewis lung carcinoma, and H460M2 human lung cancer, reduces lung metastasis weight by 71−90% and metastasis number by 40−60% in the absence of a corresponding action at the site of primary tumor growth.[54,55] The removal of only the metastatic cells from the primary tumor may explain the modest activity of NAMI-A at the primary tumor level, where these cells often represent a small fraction.[56]

Pharmacokinetic Study with 1. A pharmacokinetic study in healthy Swiss CD-1 mice was carried out to determine the fate of **1** after ip administration. The content of ruthenium in the blood, plasma, and in some organs (liver, kidney, spleen, and lung) was examined to define the fundamental pharmacokinetic parameters of **1**. The amount of ruthenium was measured, in three separate mice per group per time, by AAS after the different ip treatment schedule of **1**. Two groups received a total dose of 400 mg/kg administrated with a different frequency: the first group received 4 doses of 100 mg/kg every 2 days (days 1, 3, 5, and 7) and the other one 2 doses of 200 mg/kg with 4 days of interval (days 3 and 7). The last treated group received a single ip treatment of 200 mg/kg.

Table 6. Pharmacokinetic Data[a] for a Monocompartment Distribution

compd	treatment groups	$T_{1/2}$ (h)	V_d (mL)	Cl_{tot} (mL/h)	AUC (mg·h/L)
RAPTA-C	4 × 100 mg/kg/day	10.39	100	6.5	615
	2 × 200 mg/kg/day	12.21	163	9.2	873
	1 × 200 mg/kg	11.47	153	9.0	891
NAMI-A[b]	1 × 200 mg/kg	12.00	110	7.33	689

[a] Data were obtained by determination of **1** plasma concentrations. [b] Pharmacokinetics parameters of NAMI-A compound from ref 67.

The determination of **1** in plasma was used to calculate $T_{1/2}$, V_d, Cl_{tot}, and AUC with a monocompartment model, and the results are listed in Table 6. The half-life time ($T_{1/2}$) varies between 10.39 and 12.21 h as a function of the treatment schedule used. The distribution volumes (V_d) are between 100 and 163 mL depending on the dose. The total clearance (Cl_{tot}), that is, the volume of blood cleared of the drug by the various elimination processes (metabolism and excretion) per unit time, lies between 6.5 and 9.2 mL/h. The area under plasma concentration vs the time curve (AUC), an estimation of bioavailability and total clearance of the drugs, is between 615 and 891 mg·h/L. The results obtained with **1** seem to be influenced mostly by the last administrated dose rather than the cumulative doses. Effectively, if the values obtained with the single and repeated dose of 200 mg/kg are compared, it can be seen that the parameters are similar for these two different schedules of treatment. RAPTA-C **1** pharmacokinetic parameters can be also compared to the antimetastatic agent, NAMI-A given iv at 200 mg/kg;[57] these results are similar to those obtained with **1** given at 4 × 100 mg/kg/day. If the comparison is made between 200 mg/kg of NAMI-A and 200 mg/kg (last administration) of **1**, the results indicate that the volume of distribution and the total clearance are higher for **1**. This indicates that **1** has a better tissue penetration and a higher blood clearing than NAMI-A.

The concentration of **1** in the different organs as a function of the time after the last administration is shown in Figure 7. Ruthenium retained by the body (as the sum of the quantities found in the tested organs and the blood) 1 h after the last injection represents about 8−14% of the administrated dose depending on the dose of the treatment. It might be hypothesized that the biggest part of the administrated dose was eliminated by urine while a minor part is probably present in other body districts that were not analyzed. These percentages of ruthenium recovered in the body can be compared to the retention of the antimetastatic NAMI-A compound. When this latter compound is administrated in a single iv treatment of 200 mg/kg, the amount of recovered ruthenium 1 h after the last treatment is around 20% of the administrated dose and drops to 10% after 24 h.[57] The retention of NAMI-A is slightly higher than **1**, but

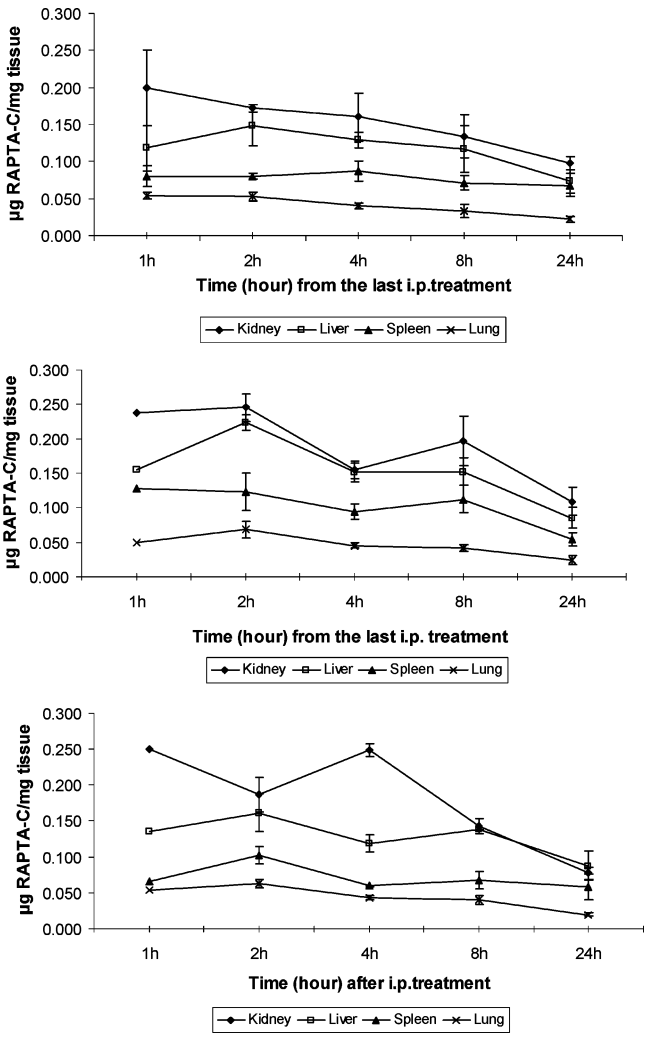

Figure 7. Concentration of **1** in the organs of mice treated ip with 4 × 100 mg/kg/day (top), 2 × 200 mg/kg/day (middle), and 1 × 200 mg/kg/day (bottom). The mice were killed by a sublethal dose of ethyl uretane at $t = 1, 2, 4, 8$, and 24 h. Data are expressed as the mean ± SE of individual samples obtained from three independent mice.

Table 7. $T_{1/2}$ of Elimination of **1** from Liver, Kidney, Spleen, and Lung of Swiss CD1-mice

treatment groups	$T_{1/2}$[a] (h)			
	liver	kidneys	spleen	lung
4 × 100 mg/kg/day	26.09	25.10	83.29	18.28
2 × 200 mg/kg/day	21.38	22.00	19.37	18.48
1 × 200 mg/kg	32.41	14.19	61.19	15.09

[a] $T_{1/2}$ was calculated according to the formula $0.693/K_e$, where K_e is the constant of elimination and obtained by linear interpolation of the ln of RAPTA-C concentration vs time.

it is interesting to look separately at the tested organs to compare the amount found in the different parts.

The measurement of the elimination rate of **1** by the organs was determined also by AAS, and the values are reported in Table 7. Complex **1** is eliminated from the lungs at a rate faster than that from the other organs tested (see Table 7). NAMI-A complex stays longer in the lung, and the slower release of this antimetastatic agent can be attributed to its binding to extracellular matrix collagen.[52] Unexpectedly, the results indicate a slow rate of elimination of **1** from the spleen.

To conclude, it is worth making a general comparison of the RAPTA compounds with NAMI-A, since NAMI-A is showing promise in clinical trials. From a structural and chemical viewpoint the compounds are very different, albeit that they are based on ruthenium. Their oxidation states differ as do their ligand sets, RAPTA being organometallic and NAMI-A a traditional coordination compound. However, in vitro cell studies show distinct similarities, and on the basis of these similarities in vivo experiments were performed. Neither types of compounds are active against primary tumors, but both reduce the number and weight of metastasis cells, with NAMI-A being slightly more effective. However, the clearance rate of **1** is slightly superior to NAMI-A which on balance suggests that the RAPTA compounds are viable for entry into clinical trials, and experiments continue.

Experimental Section

Synthesis and Chemical Characterization. The PTA ligand, its methyl derivative,[58] $[RuCl_2(arene)]_2$,[59−61] $[RuCl_2(C_6H_5(CH_2)_2Im)]_2$,[62] and $[RuCl_2(\eta^6\text{-}C_{10}H_{14})(PTA)]$[35] **1** were prepared as described previously. All of the other chemicals were obtained from Sigma unless indicated otherwise. UV−vis spectra were obtained on a JASCO V-550 or SpectraCount Packard spectrophotometer. ^1H and ^{31}P NMR spectra were recorded at 400 MHz on a Bruker Avance DPX spectrometer at room temperature in DMSO or $CDCl_3$. Electrospray ionization mass spectra were obtained on a Thermofinigan LCQ Deca XP Plus quadrupole ion trap instrument set in positive mode (solvent, methanol; flow rate, 5 µL/min; spray voltage, 5 kV; capillary temperature, 100 °C; capillary voltage, 20 V) using a literature method.[63] Chloride ion concentrations were determined with a Dionex ICS 90 ion chromatograph, using two columns (3 mm × 30 mm) IonPac AG14A and (3 mm × 150 mm) IonPac AS14A, with a suppressor MMS III, and a conductometric detector DS5. All of the solutions were prepared in double distilled water (R >12 MΩ). Calibration was conducted with 1−10 mM NaCl solutions. Elution: 0.5 mL/min, 8.0 mM Na_2CO_3/1.0 mM $NaHCO_3$.

Synthesis of $RuCl_2(\eta^6\text{-arene})(PTA)$. Compounds **3**, **5**, **8**, and **9** were prepared as follows: A methanolic solution (70 mL) of $[RuCl_2(\eta^6\text{-arene})]_2$ (0.64 mmol) and PTA (1.28 mmol) was heated to reflux for 24 h under nitrogen. The solution was allowed to cool to room temperature and filtered, and then the solvent was removed under vacuum to obtain the red-brown product (85−95%). Spectroscopic and analytical data are provided in the Supporting Information.

$RuCl_2(\eta^6$-benzo-15-crown-5)(PTA) 6. A mixture of $[RuCl_2(\eta^6\text{-benzo-15-crown-5})]_2$ (140 mg, 0.16 mmol) and PTA (50 mg, 0.32 mmol) was dissolved in chloroform and stirred at room temperature for 15 min. The solution was concentrated, and then diethyl ether was added to afford **6** as an orange solid. Yield: 165 mg (86%). Spectroscopic and analytical data is provided in the Supporting Information.

$[RuCl_2(\eta^6\text{-}C_6H_5(CH_2)_2Im)(PTA)][BF_4]$ 7. A mixture of $[RuCl_2(\eta^6\text{-}C_6H_5(CH_2)_2Im)]_2[BF_4]_2$ (150 mg, 0.16 mmol) and PTA (51 mg, 0.32 mmol) in *N*,*N*-dimethylformamide (8 mL) was heated to 50 °C for 10 min and then allowed to cool to room temperature while stirring. The solution was concentrated and diethyl ether was added which resulted in the precipitation of the product, which was washed with CH_2Cl_2 to afford **7** as an orange solid. Yield: 185 mg (92%). Spectroscopic and analytical data are provided in the Supporting Information.

Synthesis of $[RuCl_2(\eta^6\text{-arene})(Me\text{-}PTA)]Cl$. Compounds **2** and **4** were prepared as follows: A mixture of $[RuCl_2(\eta^6\text{-arene})]_2$ (0.163 mmol) and [PTA-Me]Cl (0.326 mmol) was heated to reflux under nitrogen in MeOH (25 mL) for 4 h. After evaporation of the solvent under vacuum, the residue was washed with ether (2 × 5 mL) and recrystallized from hot methanol. The product was obtained as orange crystals (80−

90%). Spectroscopic and analytical data are provided in the Supporting Information.

Thermal Denaturation. Thermal denaturation experiments were performed in quartz cuvettes. Calf thymus DNA (purchased from Sigma, St. Louis, MO) was dissolved in 10 mM phosphate buffer containing 50 mM $NaClO_4$. The ruthenium compound was added to DNA at a concentration which gave a drug to DNA ratio of 1:1. The melting curves of DNA were recorded by measuring the increase in absorbance at 260 nm from 50 to 90 °C.

Determination of pK_a Values. The pH values of NMR samples in D_2O were measured at 298 K, directly in the NMR tube, using a 713 pH meter (Metrohm) equipped with an electrode calibrated with buffer solutions at pH values of 4, 7, and 9. The pH values were adjusted with dilute HCl and NaOH. The pH titration curves were fitted to the Henderson−Hasselbalch equation using the program Micromath Scientist (Micromath Scientifc Software Inc.) with the assumption that the observed chemical shifts are weighted averages according to the populations of the protonated and deprotonated species. The resonance frequencies change smoothly with pH between the chemical shifts of the charged form HA^+, stable in acidic solution, and those of the neutral, deprotonated form A, which is present at a high pH. At any pH, the observed chemical shift is a weighted average of the two extreme values $\delta(HA^+)$ and $\delta(A)$

$$\delta_{av} = \frac{\delta(HA^+)[HA^+] + \delta(A)[A]}{[HA^+] + [A]}$$

The midpoint of the titration occurs when the concentrations of the acid and its conjugate base are equal: $[HA^+] = [A]$, that is, when the pH equals the pK_a of the compound. The pH at the midpoint of the curve is corrected by subtracting 0.44 to the pD values since the measurements were made in D_2O.[43]

In Vitro Tests. TS/A murine adenocarcinoma cell line, initially obtained from Dr. G. Forni (CNR, Centro di Immunogenetica ed Oncologia Sperimentale, Torino, Italy) belong to the tumor cell panel of the Callerio Foundation and are stored in liquid nitrogen. Cells were cultured according to a standard procedure[64] and maintained in RPMI-1640 medium (EuroClone, Wetherby, U.K.) supplemented with 10% fetal bovine serum (FBS, Invitrogen, Milano, Italy), 2 mM L-glutamine, (EuroClone, Wetherby, U.K.) and 50 μg/mL gentamycin sulfate solution (EuroClone, Wetherby, U.K.). The cell line was kept in a CO_2 incubator with 5% CO_2 and 100% relative humidity at 37 °C. Cells from a confluent monolayer were removed from flasks by a trypsin−EDTA solution (EuroClone, Wetherby, U.K.).

HBL-100, nontumorigenic human breast cells, obtained from the American Type Culture Collection, was maintained in McCoy's 5A medium (SIGMA, St. Louis, MO) supplemented with 10% FBS, 2 mM L-glutamine, 100 UI/mL penicillin, and 100 μg/mL streptomycin (EuroClone, Whetherby, U.K.) in a humidified atmosphere with 5% CO_2 at 37 °C.

Cell viability was determined by the trypan blue dye exclusion test. For experimental purposes, the cells were sown in multiwell cell culture plastic plates (Corning Costar Italia, Milano, Italy). Cell growth was determined by the MTT viability test.[65] Cells were sown on 96 well plates and after 24 h were incubated with the appropriate compound at a concentration of 1−300 μM, prepared by dissolving in a medium containing 5% of serum for 24, 48, and 72 h. Analysis was performed at the end of the incubation time. Briefly, MTT dissolved in phosphate buffered saline (PBS) (5 mg/mL) was added (10 μL per 100 μL of medium) to all wells, and the plates were then incubated at 37 °C with 5% CO_2 and 100% relative humidity for 4 h. After this time, the medium was discarded and 100 μL of DMSO (SIGMA, St. Louis, MO) was added to each well according to the method of Alley et al.[66] Optical density was measured at 570 nm on a SpectraCount Packard (Meriden, CT) instrument.

Determination of Intracellular Ruthenium. Ruthenium cell uptake was determined by AAS on samples processed using the procedure of Tamura and Arai with slight modifications.[67] For each complex tested, a six-well plate was prepared by seeding 125 000 TS/A cells in 3 mL of complete medium with 5% FBS to each experimental and control well. The plate was incubated for 24 h at 37 °C. Control wells were then washed with PBS 3 times. Control wells were filled with 3 mL of complete medium and experimental wells with 3 mL of a 100 μM solution of RAPTA compounds prepared in complete medium. The plate was incubated for 24 h at 37 °C. The wells were then washed with PBS 3 times, and the cells were collected and counted with the trypan blue exclusion test, and the intracellular concentration of ruthenium was determined. After this treatment, the cells were dried in Nalgene cryogenic vials (a first drying step was performed overnight at 80 °C and a second step at 105 °C until the samples reached a constant weight). The dried cells were decomposed by the addition of an aliquot of tetramethylammonium hydroxide (25% in water) (Aldrich Chimica, Gallarate, Milano, Italy) and of milliQ water at a ratio 1:1 directly in each vial, at room temperature, and under shaking. Final volumes were adjusted to 1 mL with milliQ water. The concentration of ruthenium in the TS/A tumor cell line was measured in triplicate by flameless AAS using a Zeeman graphite tube atomizer, model SpectrAA-300, supplied with a specific ruthenium emission lamp (hollow cathode lamp P/N 56-101447-00, Varian, Mulgrave, Victoria, Australia). Quantification of ruthenium was carried out in 10 μL samples at 349.9 nm with an atomizing temperature of 2500 °C, using argon as carrier gas at a flow rate of 3.0 L/min (for further details concerning the furnace parameter settings, see ref 19). Before each analysis, a five-point calibration curve was obtained to check the range of linearity using ruthenium custom-grade standard 998 mg/mL (Inorganic Ventures, Lakewood, NJ).

In Vivo Tests. Animal studies were carried out according to guidelines enforced in Italy (DDL 116 of 21/2/1992) and in compliance with the Guide for the Care and Use of Laboratory Animals (Department of Health and Human Services Publ. No. 86-23, Bethesda, MD, NIH, 1985).

The in vivo experiments with the RAPTA compounds were carried out with the MCa mammary carcinoma grown in CBA mice obtained from a local breeding colony grown according to the standard procedures for inbred strains. The tumor graft was carried out by injecting 10^6 cells of a cell suspension prepared from mincing with scissors the primary tumor masses obtained from donors similarly implanted 2 weeks before. The minced tissue was filtered through a double layer of sterile gauze, centrifuged at 200*g* for 10 min, and resuspended in an equal volume of PBS; viable cells were counted by the trypan blue exclusion test. These tumor cells were injected im into the calf of the left hind leg of experimental groups of mice.

Evaluation of the Primary Tumor Growth and Lung Metastases. The primary tumor growth was determined by calliper measurements, by determining two orthogonal axes, and the tumor volume was calculated with the formula: $(\pi/6)a^2b$, where a is the shorter axis and b the longer, assuming tumor density is equal to 1. The evaluation of the number and the weight of lung metastasis are performed by examining the surface of the lung immediately after sacrificing the animals by cervical dislocation. Lungs were dissected into five lobes, washed with PBS and examined under a low power microscope equipped with a calibrated grid. The weight of each metastasis was calculated by applying the same formula used for primary tumors and the sum of each individual weight gave the total weight of metastatic tumor per animal.

Pharmacokinetic Study: Determination of Ruthenium Content in the Organs, Entire Blood, and Plasma. (A). The experiment was carried out with healthy Swiss CD-1 mice purchased from Harlan Nossan (San Pietro al Natisone, Italy). Blood was obtained by intracardiac puncture after induction of anaesthesia with 1.5 g/kg ethyl uretane; an aliquot of entire blood was collected in Nalgene cryovials, and a second aliquot was centrifuged 10 min to separate the cellular fraction from the plasma. A piece of organ (liver, kidneys, lungs, spleen)

was carefully weighed and collected in Nalgene cryovials. Blood sample and organs for ruthenium determination were collected at 1, 2, 4, 8, and 24 h after the last administration.

(B) Blood and Plasma Analysis. Samples were decomposed by the addition of an aliquot of $[Me_4N][OH]$ (25% in water) (Aldrich Chimica, Gallarate, Milano, Italy) and milliQ water at a ratio of 1:1 directly in each vial, at room temperature while shaking. The samples were left at room temperature for 72 h in closed Nalgene vials until complete digestion, according to a procedure adapted from Tamura et al.[67] Final volumes were adjusted to 1 mL with milliQ water.

(C) Organ Analysis. A fragment of each organ specimen was carefully weighed and dried at 105 °C until reaching a constant dried weight in Nalgene vials. Weights were taken continuously, considering that the fragment had completely dried when no further change in weight occurred. The decomposition of the dried organs was obtained by adding an aliquot of $[Me_4N][OH]$ (25% in water) and milliQ water at a ratio of 1:1 directly in each vial, at room temperature while shaking. MilliQ water was added to give a total volume of 1 mL. Ruthenium was then determined by AAS (see above for details).

Statistical Analysis. Results were subjected to computer-assisted statistical analysis using ANOVA, Tukey−Kramer analysis of variance, and Dunnett's multiple comparison test. Differences of $P < 0.05$ were considered to be significantly different from the controls.

Acknowledgment. We thank the EPFL and COST (Switzerland) for financial support. The present work was carried out with contributions from the Laboratory for the Identification of New Antimetastasis Drugs and developed under the COST D20 action.

Supporting Information Available: Spectroscopic and analytical data for compounds **2**−**9**. This material is available free of charge via Internet at http://pubs.acs.org.

References

(1) Reedijk, J. Improved understanding in platinum antitumour chemistry. *Chem. Commun.* **1996**, (7), 801−806.
(2) Wong, E.; Giandomenico, C. M. Current status of platinum-based antitumor drugs. *Chem. Rev.* **1999**, *99*, 2451−2466 and references therein.
(3) Chu, G. Cellular responses to cisplatin. The roles of DNA-binding proteins and DNA repair. *J. Biol. Chem.* **1994**, *269*, 787−790.
(4) Cvitkovic, E.; Bekradda, M. Oxaliplatin: A new therapeutic option in colorectal cancer. *Semin. Oncol.* **1999**, *26*, 647−662.
(5) O'Dwyer, P. J.; Stevenson, J. P.; Johnson, S. W. Clinical pharmacokinetics and administration of established platinum drugs, *Drugs* **2000**, *59*, 19−27.
(6) Reedijk, J. Why does cisplatin reach guanine-N7 with competing S-donor ligands available in the cell? *Chem. Rev.* **1999**, *99*, 2499−2510 and references therein.
(7) Clarke, M. J.; Zhu, F.; Frasca, D. R. Non-Platinum Chemotherapeutic Metallopharmaceuticals. *Chem. Rev.* **1999**, *99*, 2511−2534.
(8) Guo, Z.; Sadler, P. J. Metals in Medicine. *Angew. Chem., Int. Ed. Engl.* **1999**, *38*, 1512−1531.
(9) Depenbrock, H.; Schmelcher, S.; Peter, R.; Keppler, B. K.; Weirich, G.; Block, T.; Rastetter, J.; Hanauske, A. R. Preclinical activity of trans-indazolium [tetrachlorobisindazoleruthenate (III)] (NSC 666158; IndCR.; KP 1019) against tumor colony-forming units and hematopoietic progenitor cells. *Eur. J. Cancer* **1997**, *33*, 2404−2410.
(10) Keppler, B. K.; Lipponer, K.; Stenzel, B.; Kratz, F. New tumor-inhibiting ruthenium complexes. *Met. Complexes Cancer Chemother.* **1993**, 187−220.
(11) Sava, G.; Alessio, E.; Bergamo, A.; Mestroni, G. Sulfoxide ruthenium complexes: non-toxic tools for the selective treatment of solid tumor metastases. *Top. Biol. Inorg. Chem.* **1999**, *1 (Metallopharmaceuticals I)*, 143−169.
(12) Velders, A. H.; Pazderski, L.; Ugozzoli, F.; Biagini-Cingi, M.; Manotti-Lanfredi, A. M.; Haasnoot, J. G.; Reedijk, J. Synthesis, characterization and crystal structure of trans aquatrichlorobis(5,7-dimethyl[1,2,4]triazolo[1,5-a]pyrimidine-N3)ruthenium-(III) monohydrate. *Inorg. Chim. Acta* **1998**, *273*, 259−265.
(13) Velders, A. H.; Ugozzoli, F.; Biagini-Cingi, M.; Manotti-Lanfredi, A. M.; Haasnoot, J. G.; Reedijk, J. A Unique Fourfold Intramolecular Hydrogen Bonding Stabilises the Structure of trans-Bis(2-amino-5,7-dimethyl[1,2,4]triazolo[1,5-a]pyrimidine-N3)-aquatrichlororuthenium(III) Monohydrate. *Eur. J. Inorg. Chem.* **1999**, 213−215.
(14) Hartmann, M.; Einhauser, T. J.; Keppler, B. K. Two antitumour ruthenium(III) complexes showing selectivity in their binding towards poly(dG).poly(dC) and poly(dA).poly(dT). *Chem. Commun.* **1996**, 1741−1742.
(15) Sava, G.; Bergamo, A. Ruthenium-based compounds and tumour growth control (review). *Int. J. Oncol.* **2000**, *17*, 353−365.
(16) Rademaker-Lakhai, J. M.; Van den Bongard, D.; Pluim, D.; Beijnen, J. H.; Schellens, J. H. A phase I and pharmacological study with imidazolium-trans-DMSO-imidazole-tetrachlororuthenate, a novel ruthenium anticancer agent. *Clin. Cancer Res.* **2004**, *10*, 3717−3727.
(17) Gagliardi, R.; Sava, G.; Pacor, S.; Mestroni, G.; Alessio, E. Antimetastatic action and toxicity on healthy tissues of Na-[trans-$RuCl_4$(DMSO)Im] in the mouse. *Clin. Exp. Metastasis* **1994**, *12*, 93−100.
(18) Magnarin, M.; Bergamo, A.; Carotenuto, M. E.; Zorzet, S.; Sava, G. Increase of tumor-infiltrating lymphocytes in mice treated with antimetastatic doses of NAMI-A. *Anticancer Res.* **2000**, *20*, 2939−2944.
(19) Cocchietto, M.; Sava, G. Blood concentration and toxicity of the antimetastasis agent NAMI-A following repeated intravenous treatment in mice. *Pharmacol. Toxicol.* **2000**, *87*, 193−197.
(20) Zorzet, S.; Sorc, A.; Casarsa, C.; Cocchietto, M.; Sava, G. Pharmacological effects of the ruthenium complex NAMI-A given orally to CBA mice with MCa mammary carcinoma. *Met.-Based Drugs* **2001**, *8*, 1−7.
(21) Sava, G.; Clerici, K.; Capozzi, I.; Cocchietto, M.; Gagliardi, R.; Alessio, E.; Mestroni, G. Reduction of lung metastasis by IMH-[trans-$RuCl_4$(DMSO)Im]: mechanism of the selective action investigated on mouse tumors. *Anti-cancer Drugs* **1999**, *10*, 129−138.
(22) Sava, G.; Gagliardi, R.; Bergamo, A.; Alessio, E.; Mestroni, G. Treatment of metastases of solid mouse tumors by NAMI-A: comparison with cisplatin, cyclophosphamide and dacarbazine. *Anticancer Res.* **1999**, *19*, 969−972.
(23) Sava, G.; Gagliardi, R.; Cocchietto, M.; Clerici, K.; Capozzi, I.; Marella, M.; Alessio, E.; Mestroni, G.; Milanino, R. Comparison of the effects of the antimetastatic compound ImH[trans-$RuCl_4$-(DMSO)Im] (NAMI-A) on the arthritic rat and on MCa mammary carcinoma in mice. *Pathol. Oncol. Res.* **1998**, *4*, 30−36.
(24) Keppler, B. K.; Henn, M.; Juhl, U. M.; Berger, M. R.; Niebl, R.; Wagner, F. E. New ruthenium complexes for the treatment of cancer. *Prog. Clin. Biochem. Med.* **1989**, *10*, 41−69.
(25) Kreuser, E. D.; Keppler, B. K.; Berdel, W. E.; Piest, A.; Thiel, E. Synergistic antitumor interactions between newly synthesized ruthenium complexes and cytokines in human colon carcinoma cell lines. *Semin. Oncol.* **1992**, *19*, 73−81.
(26) Srivastava, S. C.; Richard, P.; Meinken, G. E.; Larson, S. M.; Grunbaum, Z. Tumor uptake of radioruthenium compounds. In *Radiopharmaceuticals - Structure - Activity relationships*; Spencer, R. P., Ed.; Grune & Stratton Inc.: New York, 1981; pp 207−223.
(27) Sava, G.; Pacor, S.; Zorzet, S.; Alessio, E.; Mestroni, G. Antitumour properties of dimethylsulphoxide ruthenium (II) complexes in the Lewis lung carcinoma system. *Pharmacol. Res.* **1989**, *21*, 617−628.
(28) Zorzet, S.; Bergamo, A.; Cocchietto, M.; Sorc, A.; Gava, B.; Alessio, E.; Iengo, E.; Sava, G. Lack of in vitro cytotoxicity, associated to increased G2-M cell fraction and inhibition of matrigel invasion, may predict in vivo-selective antimetastasis activity of ruthenium complexes. *J. Pharmacol. Exp. Ther.* **2000**, *295*, 927−933.
(29) Clarke, M. J.; Galang, R. D.; Rodriguez, V. M.; Kumar, R.; Pell, S.; Bryan, D. M. In *Platinum and Other Metal Coordination Compounds in Cancer Chemotherapy*; Nijhoff: Boston, MA, 1988; p 582.
(30) Dale, L. D.; Tocher, J. H.; Dyson, T. M.; Edwards, D. I.; Tocher, D. A. Studies on DNA damage and induction of SOS repair by novel multifunctional bioreducible compounds. II. A metronidazole adduct of a ruthenium-arene compound. *Anti-Cancer Drug Design* **1992**, *7*, (1), 3−14.
(31) Aird, R. E.; Cummings, J.; Muir, M.; Morris, R. E.; Chen, H.; Sadler, P. J. In vitro and in vivo activity and cross resistance profiles of novel ruthenium (II) organometallic arene complexes in human ovarian cancer. *Br. J. Cancer* **2002**, *86*, 1652−1657.
(32) Morris, R. E.; Aird, R. E.; Murdoch P, D. S.; Chen, H.; Cummings, J.; Hughes, N. D.; Parsons, S.; Parkin, A.; Boyd, G.; Jodrell, D. I.; Sadler, P. J. Inhibition of cancer cell growth by ruthenium-(II) arene complexes. *J. Med. Chem.* **2001**, *44*, 3616−3621.

(33) Gopal, Y. N. V.; Jayaraju, D.; Kondapi, A. K. Inhibition of Topoisomerase II Catalytic Activity by Two Ruthenium Compounds: A Ligand-Dependent Mode of Action. *Biochemistry* **1999**, *38*, 4382−4388.
(34) Huxham, L. A.; Cheu, E. L. S.; Patrick, B. O.; James, B. R. The synthesis, structural characterization, and in vitro anti-cancer activity of chloro(p-cymene) complexes of ruthenium(II) containing a disulfoxide ligand. *Inorg. Chim. Acta* **2003**, *352*, 238−246.
(35) Allardyce, C. S.; Dyson, P. J.; Ellis, D. J.; Heath, S. L. [Ru(η^6-p-cymene)Cl_2(pta)] (pta = 1,3,5-triaza-7-phosphatricyclo[3.3.1.1]-decane): a water soluble compound that exhibits pH dependent DNA binding providing selectivity for diseased cells. *Chem. Commun.* **2001**, *15*, 1396−1397.
(36) Allardyce, C. S.; Dyson, P. J.; Ellis, D. J.; Salter, P. A.; Scopelliti, R. Synthesis and characterisation of some water soluble ruthenium(II)-arene complexes and an investigation of their antibiotic and antiviral properties. *J. Organomet. Chem.* **2003**, *668*, 35−42.
(37) Eastman, A.; Lippert, B. *Cisplatin: chemistry and biochemistry of a leading anticancer drug*; Wiley: Weinheim, Germany, 1999; p 111.
(38) Howe-Grant, M.; Lippard, S. L. *Met. Ions Biol. Syst.* **1980**, *11*, 63.
(39) Tsipis, A. C.; Sigalas, M. P. Mechanistic aspects of the complete set of hydrolysis and anation reactions of cis- and trans-DDP related to their antitumor activity modeled by an improved ASED-MO approach. *J. Mol. Struct. (THEOCHEM)* **2002**, *584*, 235−248.
(40) Bouma, M.; Nuijen, B.; Jansen, M. T.; Sava, G.; Flaibani, A.; Bult, A.; Beijnen, J. H. *Int. J. Pharm.* **2002**, *248*, 247−259.
(41) Wang, F.; Chen, H.; Parsons, S.; Oswald, I. D. H.; Davidson, J. E.; Sadler, P. J. Kinetics of Aquation and Anation of Ruthenium(II) Arene Anticancer Complexes, Acidity and X-ray Structures of Aqua Adducts. *Chem. −Eur. J.* **2003**, *9*, 5810−5820.
(42) Messori, L.; Casini, A.; Vullo, D.; Haroutiunian, S. G.; Dalian, E. B.; Orioli, P. Effects of two representative antitumor ruthenium(III) complexes on thermal denaturation profiles of DNA. *Inorg. Chim. Acta* **2000**, *303*, 282−286.
(43) Mikkelsen, K.; Nielsen, S. O. Acidity measurements with the glass electrode in H_2O-D_2O mixtures. *J. Phys. Chem.* **1960**, *64*, 632−637.
(44) Fisher, K. J.; Alyea, E. C.; Shahnazarian, N. A 31 P NMR study of the water soluble derivatives of 1,3,5-triaza-7-phosphaadamantane (PTA). *Phosphorus, Sulfur and Silicon Relat. Elem.* **1990**, *48*, 37−40.
(45) Darensbourg, D. J.; Robertson, J. B.; Larkins, D. L.; Reibenspies, J. H. Water-Soluble Organometallic Compounds. 7. Further Studies of 1,3,5-Triaza-7-Phosphaadamantane Derivatives of Group 10 Metals, Including Metal Carbonyls and Hydrides. *Inorg. Chem.* **1999**, *38*, 2473−2481.
(46) Takahara, P. M.; Frederick, C. A.; Lippard, S. J. Crystal Structure of the Anticancer Drug Cisplatin Bound to Duplex DNA. *J. Am. Chem. Soc.* **1996**, *118*, 12309−12321.
(47) Sherman, S. E.; Gibson, D.; Wang, A. H.-J.; Lippard, S. J. X-ray structure of the major adduct of the anticancer drug cisplatin with DNA: cis-[Pt(NH_3)$_2$(d(pGpG))]. *Science* **1985**, *230*, 412−417.
(48) Eastman, A. Reevaluation of interaction of cis-dichloro(ethylenediamine)platinum(II) with DNA. *Biochemistry* **1986**, *25*, 3912−3915.
(49) Fichtinger-Schepman, A. M. J.; van der Veer, J. L.; den Hartog, J. H. J.; Lohman, P. H. M.; Reedijk, J. Adducts of the antitumor drug cis-diamminedichloroplatinum(II) with DNA: formation, identification, and quantitation. *Biochemistry* **1985**, *24*, 707−713.
(50) Pil, P.; Lippard, S. *Encyclopedia of cancer*; Bertino, J. R., Ed.; 1997; p 392.
(51) Reedijk, J. The relevance of hydrogen bonding in the mechanism of action of platinum antitumor compounds. *Inorg. Chim. Acta* **1992**, *198−200*, 873−881.
(52) Sava, G.; Zorzet, S.; Turrin, C.; Vita, F.; Soranzo, M. R.; Zabucchi, G.; Cocchietto, M.; Bergamo, A.; DiGiovine, S.; Pezzoni, G.; Sartor, L.; Garbisa, S. Dual Action of NAMI-A in Inhibition of Solid Tumor Metastasis: Selective Targeting of Metastatic Cells and Binding to Collagen. *Clin. Cancer Res.* **2003**, *9*, 1898−1905.
(53) Tsien, R. Y. A nondisruptive technique for loading calcium buffers and indicators into cells. *Nature* **1981**, *290*, 527−528.
(54) Cocchietto, M.; Zorzet, S.; Sorc, A.; Sava, G. Primary Tumor, Lung and Kidney Retention and Antimetastasis Effect of NAMI-A Following Different Routes of Administration., *Invest. New Drugs* **2003**, *21*, 55−62.
(55) Sava, G.; Capozzi, I.; Clerici, K.; Gagliardi, R.; Alessio, E.; Mestroni, G. Pharmacological control of lung metastases of solid tumors by a novel ruthenium complex. *Clin. Exp. Metastasis* **1998**, *16*, 371−379.
(56) Weiss, L. Heterogeneity of Cancer Cell Populations and Metastasis. *Cancer Metastasis Rev.* **2000**, *19*, 351−379.
(57) Cocchietto, M.; Salerno, G.; Alessio, E.; Mestroni, G.; Sava, G. Fate of the antimetastatic ruthenium complex ImH [trans-$RuCl_4$-(DMSO)Im] after acute i.v. treatment in mice. *Anticancer Res.* **2000**, *20*, 197−202.
(58) Daigle, D. J.; Pepperman, A. B.; Vail, S. L. Synthesis of a monophosphorus analog of hexamethylenetetramine. *J. Heterocycl. Chem.* **1974**, *11*, 407−408.
(59) Bennett, M. A.; Smith, A. K. Arene ruthenium(II) complexes formed by dehydrogenation of cyclohexadienes with ruthenium(III) trichloride. *J. Chem. Soc., Dalton Trans.* **1974**, *2*, 233−241.
(60) Tocher, D. A.; Gould, R. O.; Stephenson, T. A.; Bennett, M. A.; Ennett, J. P.; Matheson, T. W. Areneruthenium(II) carboxylates: reactions with ligands and the X-ray structure of the p-cymene pyrazine complex [Ru(-p-$MeC_6H_4CHMe_2$)Cl$(pyz)_2$]PF_6. *J. Chem. Soc., Dalton Trans.* **1983**, *8*, 1571−1581.
(61) Zelonka, R. A.; Baird, M. C. Benzene complexes of ruthenium(II). *Can. J. Chem.* **1972**, *50*, 3063−3072.
(62) Geldbach, T. J.; Dyson, P. J. A Versatile Ruthenium Precursor for Biphasic Catalysis and Its Application in Ionic Liquid Biphasic Transfer Hydrogenation: Conventional vs Task-Specific Catalysts. *J. Am. Chem. Soc.* **2004**, *126*, 8114−8115.
(63) Dyson, P. J.; McIndoe, J. S. Analysis of organometallic compounds using ion trap mass spectrometry. *Inorg. Chim. Acta* **2003**, *354*, 68−74.
(64) Nanni, P.; De Giovanni, C.; Lollini, P. L.; Nicoletti, G.; Prodi, G. TS/A: a new metastasising cell line from BALB/c spontaneous mammary adenocarcinoma. *Clin. Exp. Metastasis* **1983**, *1*, 373−385.
(65) Mosmann, T. Rapid colorimetric assay for cellular growth and survival: application to proliferation and cytotoxicity assays. *J. Immunol. Methods* **1983**, *65*, 55−63.
(66) Alley, M. C.; Scudiero, D. A.; Monks, A.; Hursey, M. L.; Czerwinski, M. J.; Fine, D. L.; Abbott, B. J., A.; Mayo, J. G.; Shoemaker, R. H.; Boyd, M. R. Feasibility of drug screening with panels of human tumor cell lines using a microculture tetrazolium assay. *Cancer Res.* **1988**, *48*, 589−601.
(67) Tamura, H.; Arai, T. Determination of ruthenium in biological tissue by graphite furnace AAS after decomposition of the sample by tetramethylammonium hydroxide. *Bunseki Kagaku* **1992**, *41*, 13−17.

JM050015D